

ARTICLE

## Intranuclear differences in calmodulin gene expression in the trigeminal nuclei of the rat brain

Lidia Bakota<sup>1</sup>, Ivan Orojan<sup>2,3</sup>, Karoly Gulya<sup>1,4\*</sup>

<sup>1</sup>Department of Zoology and Cell Biology, University of Szeged, Szeged, Hungary, <sup>2</sup>Oncoradiology Center, Municipal Hospital, Kecskemet, Hungary, <sup>3</sup>Regional Outpatient Health Service, Kecskemet, Hungary, <sup>4</sup>Laboratory of Molecular Medicine, University of Szeged, Szeged, Hungary

**ABSTRACT** The expression patterns of the three CaM genes were quantitatively localized by using *in situ* hybridization techniques to detect gene-specific [<sup>35</sup>S]-labeled cRNA probes complementary to the multiple CaM mRNAs in the trigeminal nuclei of the adult rat brain. The three distinct CaM genes were widely expressed throughout the midbrain-brain stem area with moderate intensities. In general, mRNAs transcribed from the CaM III gene were the most abundant, followed by the CaM I and CaM II mRNA populations. Moreover, significant differences in the amounts of the transcripts of some CaM genes were found between the rostral and caudal parts of the individual nuclei of the trigeminal system. In most cases, the CaM gene-specific transcripts displayed a clear differential distribution along the rostrocaudal axis: they were more abundant in the rostral parts of these nuclei. For example, the levels of mRNAs transcribed from each of the CaM I, II and III genes were significantly higher in the rostral part of the principal sensory trigeminal nucleus, while the rostral part of the motor trigeminal nucleus exhibited an elevated amount of transcripts for the CaM I gene only. Interestingly, the CaM II mRNAs were most abundant in the caudal part of the mesencephalic trigeminal nucleus. Moreover, the largest difference between any of the CaM gene-specific transcript contents of the rostral and caudal parts was found for those of the CaM II gene in the principal sensory trigeminal nucleus. Here, the intranuclear difference was about 50%, the rostral part being the richer in CaM II mRNAs. Our results draw attention to the possible causal relation between the differences in the neuronal circuitry of the rostral and caudal parts of these nuclei and their differential CaM gene expression. This somatotopy may have important functional implications.

**Acta Biol Szeged 49(3-4):9-14 (2005)**

**KEY WORDS**

calmodulin  
gene expression  
*in situ* hybridization  
intranuclear  
mRNA  
rat  
rostrocaudal axis  
trigeminal nuclei

Calmodulin (CaM), a multifunctional cytoplasmic calcium (Ca<sup>2+</sup>) receptor protein encoded by three different genes in mammals, is especially abundant in the central nervous system (for reviews, see Palfi et al. 2002; Toutenhoofd and Strehler 2000). In our previous studies (some of them quantitative), we have already documented the regional distribution and expression pattern of the multiple CaM genes during normal development and in adulthood in the rat brain. The expression patterns corresponding to the three CaM genes displayed a widely differential distribution for the CaM gene-specific mRNA populations throughout the brain and spinal cord (Kortvely et al. 2002; Kovacs et al. 2002; Palfi et al. 1999, 2005).

As CaM exerts its biological action through its target proteins that are involved in a number of cellular regulator processes (see Kennedy 1989; Means et al. 1991; Palfi et al. 2002, for references), it is not surprising that immunohistochemical and *in situ* hybridization studies have demonstrated that CaM immunoreactivity or CaM gene-specific transcripts

are often colocalized with those of the target enzymes of CaM within the same neuronal structures, not only in general, but in the brain stem-medulla region in particular (Erondu and Kennedy 1985; Ichikawa et al. 2004; Ochiishi et al. 1998; Ogawa et al. 2005; Seto-Oshima et al. 1983; Strack et al. 1996). In the brain stem-medulla area, however, only major neuronal structures have been quantitatively analyzed so far for the CaM gene expression (Palfi et al. 1999); the finer details are still unknown. In this respect, one of the unexplored areas concerns the trigeminal nuclei that form a complex sensory and motor system with precise somatotopic organization. The afferent components of this system carry various information from the skin of the face, the oral and nasal mucosa, and deeper structures such as subcutaneous tissues, facial muscles and tendons (Waite and Tracey 1995). The head also contains several specialized structures that receive trigeminal innervation, such as the teeth and tongue, the conjunctiva and cornea, and the vibrissae, which are under voluntary motor control (Dun 1958). For rodents, the arrangement, the structure and the innervation of the facial vibrissae are similar (Rice et al. 1986), and the pattern is determined genetically (Van der Loos et al. 1984).

Accepted Dec 15, 2005

\*Corresponding author. E-mail: gulyak@bio.u-szeged.hu

Since CaM plays an important role in regulating a key target protein, Ca/CaM kinase II, in a number of neuronal functions related to the trigeminal system, including inflammation, neuropathic pain and nerve injury (Liu and Simon 2003; Ogawa et al. 2005; Price et al. 2005), a precise, high-resolution mapping of the CaM gene expression could promote a deeper understanding of the functioning of the trigeminal system in health and disease. In our present study, involving quantitative *in situ* hybridization analysis through the use of CaM gene-specific [<sup>35</sup>S]-labeled cRNA probes, we now report on the differences in CaM gene expression patterns seen along the rostrocaudal axis within each nucleus of the trigeminal system.

## Materials and Methods

### Experimental animals and tissue preparation

The experimental procedures were carried out in strict compliance with the European Communities Council Directive (86/609/EEC), and followed the Hungarian legislation requirements (XXVIII/1998 and 243/1998) regarding the care and use of laboratory animals. Five adult (200-220 g) male Sprague-Dawley rats were maintained under standard housing conditions and kept on a normal diet and tap water *ad libitum*. The animals were ether-anesthetized and decapitated between 1.00 and 3.00 p.m. The brain was quickly removed, and the brain stem-medulla area was separated, frozen and serially sectioned in a cryostat (20 µm) onto 3-aminopropyltriethoxy silane-coated glass slides and kept at -70°C until further processing (not longer than two days). The sections used in this study were cut from bregma -6.72 mm to -10.04 mm (Paxinos and Watson 1997), encompassing the entire area where the trigeminal system (mesencephalic, motor and principal sensory trigeminal nuclei) resides (see Fig. 1 for details). The spinal trigeminal nucleus was not included in this survey as its CaM gene expression pattern was weak, and did not allow an appropriate demarcation of this nucleus from other structures.

### cRNA probes

Briefly, genomic sequences of the 3'-nonhomolog regions of CaM I, II and III mRNAs were amplified by polymerase chain reactions (PCRs) as described previously (Palfi et al. 1998); sequence alignment was completed with the software BLASTN version 2.0.6 (Zhang and Madden 1997). PCRs were performed by employing EcoR I and BamH I restriction enzyme cleavage site-extended primers. The primer sequences complementary to rat genomic DNA were as follows: for CaM I, 5'-AGACCTACTTTCAACTACT, corresponding to the 30-48-bp sequence, and 5'-TGTA-AACTCATGTAGGGG, corresponding to the 236-254-bp sequence of exon 6 (Nojima and Sokabe 1987); for CaM II, 5'-ATTAGGACTCCATTCTCC, corresponding to the

144-162-bp sequence (numbered 1929-1947), and 5'-CA-CAACTCCACACTTCAACAGC, corresponding to the 353-374-bp sequence (numbered 2138-2159) of exon 5 (Nojima 1989); and for CaM III, 5'-ATGATGACTGCGAAGTGAAG, corresponding to the 12-31-bp sequence (numbered 7058-7077) of exon 6, and 5'-CAGGAGGAAGGAGAAAGAGC, corresponding to the non-transcribed genomic sequence 153-172-bp downstream to the stop codon (numbered 7228-7247; Nojima 1989). Standard PCRs were run for 35 cycles (Palfi et al. 1998), and the resulting PCR products were cloned into a pcDNA3 vector (Invitrogen Corp., Carlsbad, CA, USA) and sequenced (AB 373 DNA Sequencer, PE Applied Biosystems, Foster City, CA, USA) to confirm their identity. *In vitro* RNA syntheses from the purified and linearized vectors were carried out to prepare antisense and sense cRNA probes. For radiolabeling, [<sup>35</sup>S]UTPαS (1,100 mCi/nmol; Isotope Institute, Budapest, Hungary) was incorporated, using Riboprobe System-T7 and Riboprobe System-SP6 (Promega; Madison, WI, USA) according to the manufacturer's instructions. The complementary probe sequences were 225 bp (CaM I), 231 bp (CaM II) and 157 bp (CaM III) long. Labeled probes were purified by size exclusion chromatography. The probe-specific activities of the radiolabeled hybridizing sequences were determined to be 1.97-4.38 x 10<sup>7</sup> cpm/pmol. The specificity of the 3 antisense probes had previously been determined by sequence alignment, Northern blot analysis and *in situ* hybridization (Palfi et al. 1998, 1999).

### *In situ* hybridization

Radioactive *in situ* hybridization was carried out according to previously published protocols (Palfi et al. 1998, 1999). Briefly, coronal cryostat medullary sections were fixed for 5 min in 2x SSC containing 4% formaldehyde, washed twice in 2x SSC for 1 min, and then rinsed in 0.1 M triethanolamine containing 0.25% acetic anhydride at room temperature (RT) for 5 min. The sections were dehydrated, air-dried and then hybridized in 100 µl hybridization solution (50% formamide, 5x SSPE, 1x Denhardt's reagent, 10% dextran sulfate, 50 mM DTT, 100 µg/ml salmon sperm DNA and 100 µg/ml yeast tRNA) containing 200 fmol/ml [<sup>35</sup>S]-labeled riboprobe. The pH of the solution was adjusted to 7.4. Hybridization was performed under parafilm coverslips in a humidified chamber at 55°C for 20 h. The sections hybridized with [<sup>35</sup>S]-labeled riboprobes were extensively rinsed in 2x SSC/50% formamide at 50°C, treated with 16 µg/ml RNase A at 37°C for 30 min, washed again several times in 2x SSC/50% formamide at 50°C, and then dehydrated, air-dried and processed for autoradiography.

### Autoradiography and image analysis

Tissue sections hybridized with radioactive riboprobes were exposed to Kodak BioMax MR-1 films (Eastman Kodak Co., Rochester, NY, USA) for 5 days at -20°C and developed. At

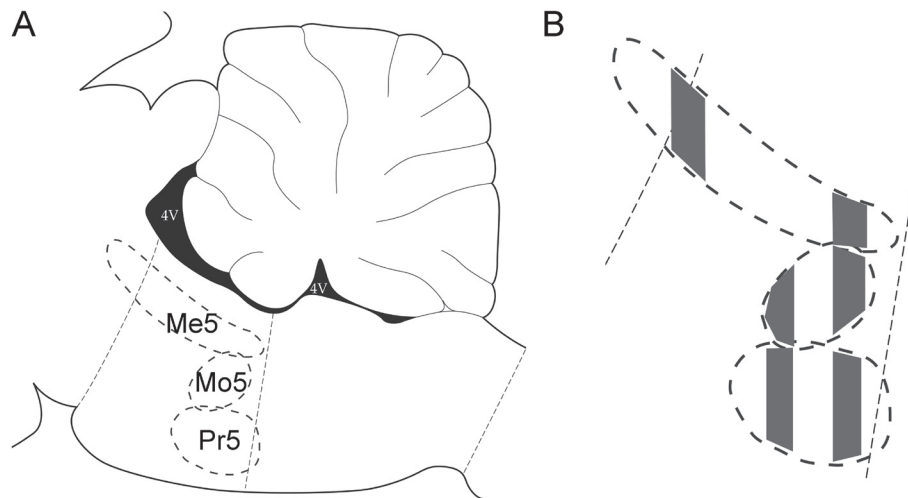


**Figure 1.A)** Schematic representation of the trigeminal nuclei (ovals outlined with dashed lines) in a section of the rat brain cut in a sagittal plane. Me5: mesencephalic trigeminal nuclei, Mo5: motor trigeminal nuclei, Pr5: principal sensory trigeminal nucleus, 4V: fourth ventricle. Note that these nuclei reside in different sagittal planes, and are never seen together as in this scheme (see Figure 2 A and B). **B)** Enlarged schematic view of the trigeminal nuclei. The tissue sections (vertical areas shaded light gray) used for analysis in this study were cut from bregma -7.64 to -7.80 for the rostral, and -9.30 to -9.68 for the caudal part of Me5, from bregma -8.80 to -9.16 for the rostral, and -9.30 to -9.68 for the caudal part of Pr5, and from bregma -8.80 to -9.16 for the rostral, and -9.30 to -9.68 for the caudal part of Mo5 (coordinates according to Paxinos and Watson (1997)). The portion of Me5 that resides more rostral than indicated here is not suitable for the measurement of CaM gene expression because the cells cannot be grouped together with certainty.

least three separate hybridization experiments for each animal were carried out for each CaM gene, and the gray-scale values for each CaM gene were measured in at least three consecutive sections. Autoradiographic images of hybridized sections were scanned at 600 x 600 dpi resolution and analyzed by the computer program Image J (version 1.32; developed at the U.S. National Institutes of Health by W. Rasband, and available from the Internet at <http://rsb.info.nih.gov/ij>). Regions of interests within the trigeminal system were outlined on the computer screen and their signal intensities were measured. It is important to note that some parts of the trigeminal nuclei cannot be delineated properly on the basis of the autoradiographic distribution of their CaM gene-specific mRNA contents. Thus, for example, we were unable to discriminate between certain parts of the principal sensory trigeminal nucleus; accordingly, gray-scale values for its dorsomedial and ventrolateral parts are not reported separately here. Gray values between 0 (lightest) and 255 (darkest) were assigned to the images, and the specific gray values were determined by subtracting the sense values from the corresponding antisense values. Analysis of significance was carried out with the two-tailed Student's *t*-test (Microsoft Excel 2004 for Mac, Ver. 11.2; Microsoft, Redmond, WA, USA).

## Results

*In situ* hybridization of [<sup>35</sup>S]-labeled antisense CaM I, II and III cRNA probes to tissue sections of the brain stem-medulla region established a specific and unique distribution of the

autoradiographic label (Fig. 2), whereas hybridization with a sense probe (not shown) resulted in a very low labeling with nonspecific distribution. CaM mRNAs transcribed from the three CaM genes were widely distributed, albeit generally with low-to-medium levels, throughout this brain area. Quantitative image analysis of the autoradiograms revealed that mRNAs transcribed from the CaM III gene were generally most abundant, followed by CaM I and CaM II mRNA populations (Table 1). This rank order of signal intensity is identical to that reported for other brain (Palfi et al. 1999) and spinal cord areas (Kovacs and Gulya 2002). The highest specific optical density was detected in the motor trigeminal nucleus for CaM III transcripts, and the smallest one in the principal sensory trigeminal nucleus for the CaM II gene. For some CaM genes, significant differences in the amounts of their transcripts were found between the rostral and caudal parts of the individual nuclei of the trigeminal system. In most cases, the CaM gene-specific transcripts were more abundant in the rostral parts of the nuclei, as the levels of mRNAs transcribed from each of the CaM I, II and III genes were significantly higher in the rostral part of the principal sensory trigeminal nucleus, while the rostral part of the motor trigeminal nucleus displayed an elevated amount of transcripts for the CaM I gene only. For example, the levels of CaM I transcripts were about 38% and 37% higher in the rostral parts of the principal sensory trigeminal nucleus and the motor trigeminal nucleus, respectively. Interestingly, the CaM II mRNAs were most abundant in the caudal part of

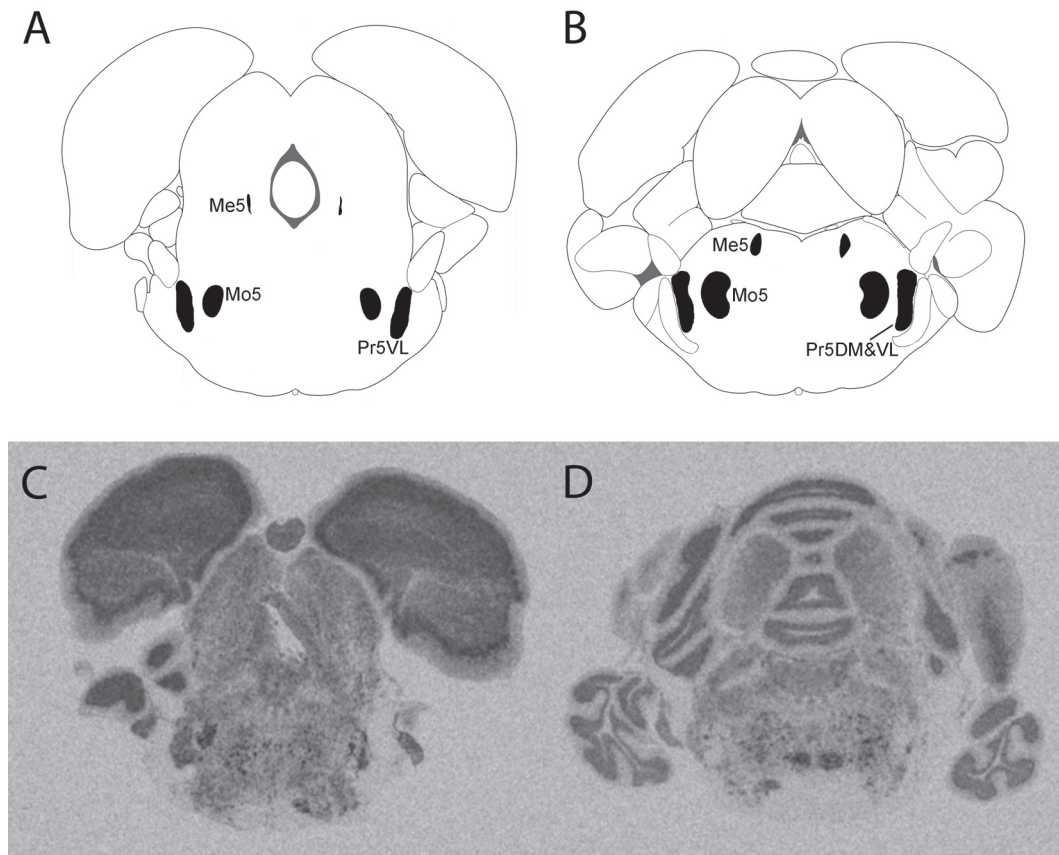


**Figure 2.** Differential CaM gene expression in the trigeminal nuclei of the rat brain, as evidenced by the specific hybridization of antisense CaM I-gene specific  $[^{35}\text{S}]$ cRNA probes. A, B) Diagrammatic representation of the medullary nuclei (areas labeled solid black) in the rat brain (Paxinos and Watson 1997). Me5: mesencephalic trigeminal nuclei, Mo5: motor trigeminal nuclei, Pr5VL: principal sensory trigeminal nucleus, ventrolateral part, Pr5DM&VL: principal sensory trigeminal nucleus, dorsomedial and ventrolateral parts. C, D) Specific hybridization of antisense CaM I-gene specific  $[^{35}\text{S}]$ cRNA probes to the coronal sections of the rat brain stem-medulla area. Representative pictures taken from bregma -8.80 (C) and -9.30 mm (D), respectively.

the mesencephalic trigeminal nucleus. The largest difference between any CaM gene-specific transcript contents of the rostral and caudal parts was found for the CaM II gene in the principal sensory trigeminal nucleus, where the levels of these transcripts were otherwise characteristically the lowest. The intranuclear difference here was about 50%, the rostral part being the richer in CaM II mRNAs.

## Discussion

Among the cranial nerves that carry sensory information to the central nervous system, the rodent trigeminal system is of special interest because of its precise somatotopic organization (Waite 1984; Waite and Tracey 1995). The trigeminal sensory nuclei are divided into three groups: the mesencephalic nucleus (Me5), the principal sensory nucleus (Pr5), and the spinal trigeminal nucleus (Sp5), this latter being subdivided into the nucleus spinal subnuclei oralis (Sp5O), the nucleus interpolaris (Sp5I) and the nucleus caudalis (Sp5C). The

organization of terminations in the main and spinal nuclei is most clearly evident for vibrissal afferents, for which a pattern analogous to the peripheral arrangement of vibrissae can be discerned in coronal sections. Each vibrissa is associated with a patch or barrel (for references, see Waite and Tracey 1995). In general, three representations of the vibrissae are seen, in Pr5, Sp5I and Sp5C; although Sp5O receives vibrissal terminations, no patches are evident in this subnucleus. In the horizontal plane, terminations from each vibrissa are seen as long rostrocaudal columns throughout the nuclei in a somatotopic pattern. The presence of the somatotopic pattern of the rostrocaudal barrels is most evident for the principal sensory nucleus. Our CaM expression data here could be interpreted as showing a differential CaM mRNA distribution along the rostrocaudal axis of this nucleus, which is a consequence of the separate information received from the rostral and caudal vibrissal fields.

The motor trigeminal nucleus of the rat is divided into a large dorsolateral division extending throughout the ros-

**Table 1.** Quantitative analysis of CaM gene expression in the trigeminal nuclei of the adult rat brain.

Component of the trigeminal system	Gene	Average specific gray-scale value ( $\pm$ S.D.)		% of rostral value caudal
		rostral	caudal	
Mesencephalic trigeminal nucleus	CaM I	63.28 $\pm$ 11.79	64.27 $\pm$ 6.95	98.46
	CaM II	56.12 $\pm$ 6.67	73.33 $\pm$ 8.09*	76.53
	CaM III	86.31 $\pm$ 19.64	60.21 $\pm$ 8.20	143.35
Principal sensory trigeminal nucleus	CaM I	76.78 $\pm$ 6.85	55.78 $\pm$ 9.33*	137.65
	CaM II	43.17 $\pm$ 7.72	28.86 $\pm$ 3.70*	149.58
	CaM III	80.87 $\pm$ 5.10	66.97 $\pm$ 6.69*	120.76
Motor trigeminal nucleus	CaM I	79.02 $\pm$ 7.48	57.48 $\pm$ 9.84*	137.47
	CaM II	38.62 $\pm$ 7.55	42.13 $\pm$ 6.23	91.67
	CaM III	88.22 $\pm$ 6.85	77.26 $\pm$ 8.06	114.19

Coronal cryostat sections from the pons-medulla area were cut, hybridized separately with antisense [<sup>35</sup>S]cRNA probes specific for CaM I, CaM II or CaM III mRNAs and exposed to autoradiographic film. Film autoradiographic images (at least 4 in each of the 5 animals for a given structure) were analyzed by computer-assisted microdensitometry. Gray-scale levels for each CaM gene were determined by using the image analysis computer program Image J (ver. 1.32). High-resolution gray-scale images were taken and the brain stem structures of interest were outlined on the computer screen. Specific gray-scale values (means of at least 20 measurements from 5 separate experiments  $\pm$  S.D.) were calculated by subtracting the nonspecific values resulting from the hybridization of the respective sense cRNA probes from the values of the antisense [<sup>35</sup>S]cRNA probes. \*Significant differences ( $p < 0.05$ , two-tailed Student's *t*-test) were found between the rostral and caudal parts of the trigeminal nuclei.

trocaudal length of the nucleus and a smaller ventromedial division in the caudal two-thirds (for references, see Travers 1995). The jaw closing muscles, the masseter, the temporalis and the medial pterygoid, are innervated from the dorsolateral division, while two jaw opening muscles, the anterior digastric and the mylohyoid, are innervated from the ventrolateral division. A third jaw opening muscle, the lateral pterygoid, is grouped together with jaw closing motoneurons in the ventral aspect of the dorsoventral division. Even though the areas corresponding to the dorsolateral and ventromedial divisions are not distinguishable on the basis of their CaM gene expression patterns in the coronal sections of the caudal part of the nucleus, the caudal part nevertheless clearly has higher levels of CaM mRNA populations.

The major organizing principles of the vertebrate central nervous system determine that its parts receive inputs from separate sources, while separate efferent connections project to different neuroanatomical entities. Previous studies have established that certain nuclei in the central nervous system display a differential structural and functional organization, mainly along their rostrocaudal axis, that can be seen in the differences in their neuronal circuitry, neurochemical cytoarchitecture or gene expression pattern. This somatotopy is also present in the brain stem, one of the nuclei most characteristically expressing this feature being the parabrachial nucleus (PBN). The PBN has been divided into at least 13 distinct subnuclei and regions, each associated with a unique set of afferents, efferents and neurotransmitters (for references, see Saper 1995), which frequently mark out distinct terminal fields according to their receptive fields. For example, projections to the PBN from the nucleus of the solitary tract carry afferent signals from both the oral cavity and the gastrointestinal tract. Although physiological studies have suggested

the convergence of oral and gastrointestinal sensory signals in the PBN, anatomical studies have emphasized the segregation of these pathways in the rat. Karimnamazi et al. (2002) found that the gastric terminations in the PBN were separate from the taste projections in the rostral portion of the external lateral and dorsal lateral subnuclei, while the gustatory projections were separate from the gastric terminations in the ventral lateral and central medial subnuclei of the caudal "waist" region, and were intermingled with the gastric projections in these subnuclei and the external subnuclei at slightly more rostral levels. The physiological evidence for overlap in the PBN was also evaluated, as neurophysiological recordings demonstrated that a small proportion of single cells within the waist and external subnuclei could be activated by both gastric and orotactile stimulation. The behavioral roles of the "waist" area and external subnuclei of the PBN in the processing of gustatory information have also been defined by monitoring oromotor behavior in the areas within and surrounding this nucleus (Galvin et al. 2004). Electrical and chemical stimulation of the "waist" area increased ingestive oromotor behavior, while stimulation of the external parabrachial subnuclei and areas medial and ventral to the nucleus did not result in a behavioral change. These data supported the hypothesis that the waist area of the PBN constitutes part of the neural substrate involved in eliciting oromotor behavior in response to taste input. However, another experiment (Gulya et al. 1991) provided indirect evidence for the separation of functions within a nucleus that resides outside the brain stem. It was reported that the vasopressin-containing cells in the bed nucleus of the stria terminalis responded to dehydration and/or to ethanol treatment in a subregion-dependent manner within the nucleus. Dehydration affected only cells in the central (or medial) region, while ethanol ingestion also

affected cells in the caudal region of the nucleus. As the different parts of this nucleus send afferents both to the lateral septum and to the neurohypophysis in rodents (Kelly and Swanson 1980), or to several regions of the mesencephalon, pons and medulla oblongata in the cat (Holstege et al. 1985), the anatomical basis for the segregation of functions, involving the differential regulation of vasopressin gene expression, is plausible.

In summary, our results draw attention to a possible causal relation between the differences in afferent and efferent neuronal connections (and consequently in their presumably segregated functions) of the rostral and caudal parts of the trigeminal nuclei and their differential CaM gene expression.

## Acknowledgments

This research was supported by grants from the National Scientific Research Fund, Hungary (T034621) and from the Regional Neurobiology Knowledge Center (RET006) to K.G. We thank Mrs. Susan Ambrus for her excellent technical help.

## References

Dun RB (1958) Growth of the mouse coat. *Aust J Biol Sci* 11:95-105.

Erondu NE, Kennedy MB (1985) Regional distribution of type II Ca<sup>2+</sup>/calmodulin-dependent protein kinase in rat brain. *J Neurosci* 5:3270-3277.

Galvin KE, King CT, King MS (2004) Stimulation of specific regions of the parabrachial nucleus elicits ingestive oromotor behaviors in conscious rats. *Behav Neurosci* 118:163-172.

Gulya K, Dave JR, Hoffman PL (1991) Chronic ethanol ingestion decreases vasopressin mRNA in hypothalamic and extrahypothalamic nuclei of mouse brain. *Brain Res* 557:129-135.

Holstege G, Meiners L, Tan K (1985) Projections of the bed nucleus of the stria terminalis to the mesencephalon, pons, and medulla oblongata in the cat. *Exp Brain Res* 58:379-391.

Ichikawa H, Gouty S, Regalia J, Helke CJ, Sugimoto T (2004) Ca<sup>2+</sup>/calmodulin-dependent protein kinase II in the rat cranial sensory ganglia. *Brain Res* 1005:36-43.

Karimnamazi H, Travers SP, Travers JB (2002) Oral and gastric input to the parabrachial nucleus of the rat. *Brain Res* 957:193-206.

Kelly J, Swanson LW (1980) Additional forebrain regions projecting to the posterior pituitary: preoptic region, bed nucleus of the stria terminalis, and zona incerta. *Brain Res* 197:1-9.

Kennedy MB (1989) Regulation of neuronal function by calcium. *Trends Neurosci* 12:417-420.

Kortvely E, Palfi A, Bakota L, Gulya K (2002) Ontogeny of calmodulin gene expression in rat brain. *Neurosci* 114:301-316.

Kovacs B, Gulya K (2002) Differential expression of multiple calmodulin genes in cells of the white matter of the rat spinal cord. *Mol Brain Res* 102:28-34.

Liu L, Simon SA (2003) Modulation of IA currents by capsaicin in rat trigeminal ganglion neurons. *J Neurophysiol* 89:1387-1401.

Means AR, VanBerkum MF, Bagchi I, Lu KP, Rasmussen CD (1991) Regulatory functions of calmodulin. *Pharmacol Ther* 50:255-270.

Nojima H (1989) Structural organization of multiple rat calmodulin genes. *J Mol Biol* 208:269-282.

Nojima H, Sokabe H (1987) Structure of a gene for rat calmodulin. *J Mol Biol* 193:439-445.

Ochiishi T, Yamauchi T, Terashima T (1998) Regional differences between the immunohistochemical distribution of Ca<sup>2+</sup>/calmodulin-dependent protein kinase II alpha and beta isoforms in the brainstem of the rat. *Brain Res* 790:129-140.

Ogawa A, Dai Y, Yamanaka H, Iwata K, Niwa H, Noguchi K (2005) Ca<sup>2+</sup>/calmodulin-protein kinase IIalpha in the trigeminal subnucleus caudalis contributes to neuropathic pain following inferior alveolar nerve transection. *Exp Neurol* 192:310-319.

Palfi A, Hatvani L, Gulya K (1998) A new quantitative film autoradiographic method of quantifying mRNA transcripts for *in situ* hybridization. *J Histochem Cytochem* 46:1141-1149.

Palfi A, Kortvely E, Fekete E, Gulya K (2005) Multiple calmodulin mRNAs are selectively transported to functionally different neuronal and glial compartments in the rat hippocampus. An electron microscopic *in situ* hybridization study. *Life Sci* 77:1405-1415.

Palfi A, Kortvely E, Fekete E, Kovacs B, Varszegi S, Gulya K (2002) Differential calmodulin gene expression in the rodent brain. *Life Sci* 70:2829-2855.

Palfi A, Vizi S, Gulya K (1999) Differential distribution and intracellular targeting of mRNAs corresponding to the three calmodulin genes in rat brain: a quantitative *in situ* hybridization study. *J Histochem Cytochem* 47:583-600.

Paxinos G, Watson C (1997). *The rat brain in stereotaxic coordinates*, 3rd ed. Academic Press, San Diego.

Price TJ, Jeske NA, Flores CM, Hargreaves KM (2005) Pharmacological interactions between calcium/calmodulin-dependent kinase II alpha and TRPV1 receptors in rat trigeminal sensory neurons. *Neurosci Lett* 389:94-98.

Rice FL, Manse A, Munger BL (1986) A comparative light microscopic analysis of sensory innervation of the mystacial pad. I. Innervation of vibrissal follicle-sinus complexes. *J Comp Neurol* 252:154-174.

Saper CB (1995) Central autonomic system. In *The rat nervous system*. ed., Paxinos G. Second ed. Academic Press, San Diego, pp. 107-135.

Seto-Ohshima A, Kitajima S, Sano M, Kato K, Mizutani A (1983) Immunohistochemical localization of calmodulin in mouse brain. *Histochem* 79:251-257.

Strack S, Wadzinski BE, Ebner FF (1996) Localization of the calcium/calmodulin-dependent protein phosphatase, calcineurin, in the hindbrain and spinal cord of the rat. *J Comp Neurol* 375:66-76.

Toutenhoofd SL, Strehler EE (2000) The calmodulin multigene family as a unique case of genetic redundancy: multiple levels of regulation to provide spatial and temporal control of calmodulin pools? *Cell Calcium* 28:83-96.

Travers JB (1995) Oromotor nuclei. In *The rat nervous system*. ed., Paxinos G. Second ed. Academic Press, San Diego, pp. 239-255.

Van der Loos H, Dorfl J, Welker E (1984) Variation in pattern of mystacial vibrissae in mice. *J Hered* 75:326-336.

Waite PME (1984) Rearrangement of neuronal responses in the trigeminal system of the rat following peripheral nerve section. *J Physiol (Lond)* 352:425-445.

Waite PME, Tracey DJ (1995) Trigeminal sensory system. In *The rat nervous system*. ed., Paxinos G. Second ed. Academic Press, San Diego, pp. 705-724.

Zhang J, Madden TL (1997) PowerBLAST: new network BLAST application for interactive or automated sequence analysis and annotation. *Genome Res* 7:649-656.